PORE-WATER PRESSURES IN EARTH SLOPES UNDER SEISMIC LOADING CONDITIONS

by

H. Bolton Seed[I] and Kenneth L. Lee[II]

Introduction

Analyses of stability problems involving soils can be made in terms of either total or effective stresses. Normally effective stress analyses are preferred but their use requires a reliable evaluation of the distribution of pore-water pressures in the soil mass under consideration. The determination of pore-water pressures in earth slopes during earthquakes presents a particularly difficult problem and for this reason, total stress methods are often used for analysis purposes. The present paper discusses some of the difficulties in evaluating pore-water pressures for seismic design studies.

It has long been recognized that the ground vibrations induced by earthquakes can lead to large increases in pore-water pressures in soils, as evidenced by the number of cases of soil liquefaction and flow slides which have occurred during earthquakes (1). Under level ground conditions, it would appear that the stress conditions induced in soil elements in the ground can be reproduced with reasonable accuracy in the laboratory by means of cyclic loading simple shear tests. Idealized loading conditions for a soil element in the ground are shown in Fig. 1 and the pore pressures and deformations induced in such an element of saturated sand in a cyclic loading simple shear test (2) are shown in Fig. 2. The progressive increase in pore-water pressure in the soil is readily apparent. Stress conditions of this type cannot be reproduced in laboratory triaxial compression tests, though they can be approximated (3). Thus unless appropriate corrections are made (2,4), triaxial test procedures can lead to substantial discrepancies in evaluations of soil behavior.

In an earth slope, however, soil elements are subjected to appreciable pre-earthquake shear stresses on potential failure surfaces and under these conditions the stress conditions induced during earthquakes can be reproduced with reasonable accuracy by triaxial test procedures. There is some evidence that this will be the case whenever the initial shear stress conditions on a failure plane are reproduced by a principal stress ratio exceeding about 1.5 in a triaxial compression test. It was to investigate the development of pore-water pressures under these conditions that the following studies were conducted.

I. Professor of Civil Engineering, University of California, Berkeley, California.

II. Assistant Professor of Engineering, University of California, Los Angeles, California.

Pore Pressures During Cyclic Load Tests on Anisotropically-Consolidated Samples of Saturated Sand

The application of pre-earthquake stresses on a potential failure surface in a laboratory test specimen is most easily achieved in triaxial compression tests by consolidating the sample under anisotropic stress conditions. The cyclic stresses induced by an earthquake are then simulated by superimposing a cyclic deviator stress on the initial stress condition.

The results of such a test performed on a sample of sand having an initial relative density of 50 percent are shown in Fig. 3. The sample was first consolidated under an effective minor principal stress of 4 kg per sq cm and an effective major principal stress of 8 kg per sq cm to an effective principal stress ratio of 2. The sample was then subjected, under undrained loading conditions, to a cyclic deviator stress of 3.8 kg per sq cm. The cyclic deviator stress was selected to have this relatively large value in order to produce a failure condition at some stage in the test. The resulting changes in pore-water pressure, effective principal stress ratio and axial strain with time are shown in Fig. 3.

For purposes of comparison the results of a static load undrained test on the same sand under the same initial stress conditions are shown in Fig. 4. It may be seen that the maximum effective principal stress ratio at failure is about 3.6 and the pore-water pressure under a deviator stress of 8 kg per sq cm is about 0.6 kg per sq cm.

Under the cyclic load conditions shown in Fig. 3, the sample behaves during the first loading as it would in a static load test. However beyond this stage the pore pressures follow a cyclic pattern related to the cyclic stress applications. The maximum pore-water pressure during any one cycle increases progressively but the minimum pore-water pressure remains essentially constant. A careful study of the data in Fig. 3 shows that during any one cycle the maximum pore-water pressure develops when the deviator stress is about equal to zero and that the minimum pore-water pressure develops when the deviator stress reaches its maximum value.

Of particular interest however are the high values of the effective principal stress ratios developed during the test. It is clear that on an effective stress basis, the effective principal stress ratio reaches a failure condition during each cycle after the second. However large strains do not develop in the specimen due to the fact that the failure condition persists for such a short time that no significant deformations can occur. However each time the cyclic stress is increased a failure condition is developed for a very short period of time and a small additional deformation occurs in the test specimen. As the loading continues the total strain accumulates, but even though the specimen has reached a failure condition a number of times the total deformation remains relatively small.

In effect the pore-water pressure appears to adjust, once the failure condition has developed, to keep the effective principal stress ratio at its failure value. Thus even though the deviator stress continues to build up after the critical effective principal stress ratio has developed, the pore-water pressure decreases to maintain the effective principal stress ratio at its critical value.

In the light of this type of behavior it is apparent that the period of time for which the critical effective principal stress ratio is maintained during any one cycle will determine the magnitude of the sample deformations. Thus analyses of deformations in terms of effective stresses requires not only a knowledge of the maximum pore-water pressures likely to develop but also a knowledge of the full time history of pore-water pressures in order to determine the time history of effective principal stress ratios.

Similar behavior is observed in tests conducted using higher values of the cyclic deviator stress. Fig. 5 presents the results of a similar test on the same sand using the slightly high cyclic deviator stress of 4.5 kg per sq cm. In this case the pore-water pressures reached extremely high values, becoming almost equal to the applied confining pressure at some stages in the test. However it may be seen that these high values were developed at stages where the deviator stress was very small and as the magnitude of the deviator stress increased later in the cycle, the pore-water pressure dropped to a much lower value. Again, however, the pore-water pressure developed during the loading part of the cycle was always consistent with the development of an effective principal stress ratio which was equal to or less than the critical value. In this case, however, the existence of very high pore-water pressures during the unloading part of the stress cycle resulted in the critical effective principal stress ratio being developed at a very early stage of the loading cycle and thus being maintained for a substantial part of the loading cycle. As a result of the longer duration of the 'failure' condition, much larger deformations occurred than was the case for the test data presented in Fig. 3.

A comparison of the test data in Figs. 3 and 5 with that for a third test conducted at an intermediate value of the cyclic deviator stress is shown in Fig. 6. It may be seen that in all three specimens, the values of the pore-water pressures when the deviator stress was a maximum were about the same even though they were quite different at other stages of the test. Furthermore in all specimens a failure condition developed at some stage of the loading as evidenced by the development of an effective principal stress ratio of 3.7 to 4.0. Never-the-less the samples showed quite different deformations, the axial strains in the three tests increasing in relation to the length of time, during each test, for which the critical effective principal stress ratio was maintained.

Use of Measured Pore Pressures in Effective Stress Analyses

Thus it would appear that a major problem in effective stress analyses of the behavior of saturated soils in earth slopes during earthquakes is to predict not only the magnitude of the pore-water pressures which will develop, but also the time history of the pore-water pressure changes in order to determine the periods of time for which they will be sufficiently high to produce a temporary failure condition. At the same time it must be recognized that the occurrence of such a failure condition during one or more load cycles will not necessarily lead to excessive deformations of the embankment.

The pore-water pressures developed during a static load test on a soil apparently shed little light on this type of behavior. For all the tests shown in Fig. 6, the static pore-water pressures under the applied deviator stresses would have been about 0.6 kg per sq cm. Even the lowest values of the pore-water pressure developed during cyclic loading were about 65 percent higher than this while the maximum values were many times larger. While the soil behavior during the first half of the first loading cycle is consistent with the behavior during a static load test, it is apparently quite different thereafter.

The problems associated with predicting the time histories of pore-water pressures in saturated soils during earthquakes would seem to make effective stress analyses of embankment deformations extremely difficult at the present time. Until a much better understanding of the pore-water pressures developed under cyclic loading conditions is available it would therefore seem more expedient to simulate the field loading conditions as carefully as possible in laboratory tests and use total stress data as a basis for analyses of slope behavior.

Strength of Soil Under Pulsating Loading - Total Stress Basis

The basic objective of soil testing for total stress analyses is to simulate in the laboratory, as accurately as possible, the stress conditions which develop in the field. Laboratory testing of soil samples to simulate earthquake loading conditions is done in two stages. The prepared test specimens are first consolidated under static stresses similar to those existing on corresponding elements in the field. After equilibrium is attained, the drainage line is closed and the sample is then subjected to a pulsating cyclic axial stress of sufficient magnitude to cause excessive deformation within a reasonable number of cycles.

If the triaxial test is used, the consolidation stress conditions must be controlled by the chamber pressure and the piston load. These loads produce only principal stresses on the sample. Thus, for testing it is convenient to express the consolidation stress conditions in terms of the minor principal stress σ_{3c} and the principal stress ratio $K_c = \sigma_{1c}/\sigma_{3c}$. The subscript 'c' denotes that the stresses act during consolidation, and therefore at the end of the consolidation stage they are effective or intergranular stresses.

Appropriate values of the principal stresses and the principal stress ratio for use in the laboratory testing program must be determined for elements of soil at different key locations within the earth embankment to be studied. Bishop (5) found by a rigorous mathematical approach that the major principal stress, σ_1 at all locations within an embankment simulated by an elastic wedge was approximately equal to the vertical overburden pressure. Clough and Woodward (6) have studied this problem using the finite element method. In addition to confirming Bishop's findings with respect to σ_1, they also computed other components of stress. From their work it is possible to compute the principal stress ratio, K_c, at any point within an embankment simulated by an elastic wedge.

Values of K_c at different locations within an idealized homogeneous elastic embankment computed by the finite element method and taking into account the construction procedure are shown in Fig. 7. It may be seen that the principal stress ratio is approximately equal to 2 over much of the embankment with somewhat different values occurring in small regions. The values of the principal stress ratio will vary to some extent with the values of the modulus and Poisson's ratio used in the analysis. However, for most cases the value of K_c will always range between 1.5 and 2.5 over a large portion of the embankment.

Lowe and Karafiath (7) have suggested a different approach for computing the principal stress ratio to be used in connection with stability analyses of earth dams. Except for very relatively horizontal failure surfaces this method also usually leads to values of K_c within the range 1.5 to 2.5.

Thus a stability analysis will normally require a knowledge of the strength of samples of soil consolidated under major principal stresses up to a maximum value of the effective overburden pressure in the field, and under principal stress ratio conditions ranging from about 1.5 to 2.5.

The results of a series of tests performed on samples of a fine silty sand from a hydraulic fill dam consolidated under a principal stress ratio of 2 are shown in Fig. 8. The material had an in-place unit weight corresponding to a relative density of about 50 percent. The triaxial test specimens were prepared to this density, saturated using an appropriate back-pressure, and subjected to cyclic load tests similar to those illustrated in Figs. 3, 5 and 6.

The data in Fig. 8a shows the results of four tests on samples prepared and consolidated to the same conditions but subjected to different magnitudes of cyclic deviator stress; the relationships show the maximum axial strains developed as a result of increasing numbers of stress cycles. The values of σ_{df} shown in the figure represent the peak deviator stresses developed during the cyclic loading. It may be seen that for this soil the samples did not suddenly collapse; rather they developed progressive deformations which accumulated and increased with each succeeding cyclic stress application. It is necessary therefore to define failure in terms of a limiting deformation and the anticipated number of significant stress cycles for the structure and earthquake under consideration. While the actual stress pulses induced in a soil deposit are highly irregular, they can usually be represented with sufficient accuracy by an equivalent number of uniform stress cycles; for most earthquakes the number of significant cycles is likely to lie between about 5 and 30.

The failure criterion selected may be a limiting strain of 5%, 10% or 20% depending on the tolerable deformations of the soil structure during an earthquake. Having selected this criterion, the test data shown in Fig. 8a can readily be replotted to show the values of peak deviator stress required to produce this strain in different numbers of cycles, as shown in Fig. 8b. Finally, for the significant number of cycles in the earthquake under consideration (say, 10) the values of peak cyclic deviator stress causing different strains in 10 cycles may be read off from Fig. 8b and plotted as a function of the effective minor principal stress as shown in Fig. 9a. By conducting similar series of tests using the same principal stress ratio during consolidation but different values of the minor principal stress, the family of curves shown in Fig. 9a may readily be established.

Finally by performing similar test series on samples initially consolidated under different principal stress ratios, appropriate strength values for use in a total stress analysis can be determined. The results of tests on samples of the silty sand hydraulic fill initially consolidated under effective principal stress ratios of 1.0, 1.5 and 2.0 are shown in Fig. 8b; for the data in this figure a failure criterion of 20 percent strain in 10 cycles was selected.

The importance of conducting tests on samples initially consolidated under the appropriate principal stress ratio is readily apparent from the data in Fig. 9b. Consolidation of samples under an ambient pressure, corresponding to a principal stress ratio of 1, as is often done in triaxial testing of soils, could lead to a gross under-estimate of the resistance of the soil to deformation.

Similar test data for a fine to medium sand is shown in Fig. 10. In this case also, the large influence of the value of the principal stress ratio during consolidation is readily apparent.

Finally Fig. 11 shows a comparison, for the fine to medium sand, of the stresses inducing 20 percent strain in undrained cyclic loading tests, undrained static loading tests and drained static loading tests. There is no evident relationship between the strength under static loading conditions and the resistance to deformation under cyclic loading conditions (8). Thus, as indicated by the test data in Figs 3, 5 and 6, it is apparently necessary to perform cyclic loading tests in order to evaluate the strength or resistance to deformation of saturated cohesionless materials under the cyclic loading conditions induced by earthquakes.

Conclusion

Under cyclic loading conditions, the pore-water pressures in saturated cohesionless soils change progressively. Thus in order to perform an effective stress analysis it is necessary to determine not only the magnitude of the pore pressures that may develop but also the time history of pore-water pressures in order to determine the periods of time for which the soil may be brought to a temporary failure condition. The problems associated with predicting the time history of pore-water pressures would appear to make effective stress analyses of embankment deformations extremely difficult at the present time. Accordingly a method for evaluating the resistance to deformation of saturated soils subjected to cyclic loading in terms of total stresses has been presented. Development of test data of this type provides an expedient means for incorporating the data in dynamic analyses of embankment stability during earthquakes (9,10).

Acknowledgements

Many of the cyclic loading tests reported herein were performed by Mr. John A. Fitton and Mr. Henry G. Walters, graduate research assistants, University of California, Los Angeles.

References

1. Seed, H. Bolton, "Landslides During Earthquakes Due to Soil Liquefaction," Journal of the Soil Mechanics and Foundations Division, ASCE, Sept. 1968.

2. Peacock, W. H. and Seed, H. Bolton, "Sand Liquefaction Under Cyclic Loading Simple Shear Conditions," Journal of the Soil Mechanics and Foundations Division, ASCE, Vol. 94, No. SM3, May 1967, pp. 689-708.

3. Seed, H. Bolton and Lee, Kenneth L., "Liquefaction of Saturated Sands Under Cyclic Loading," Journal of the Soil Mechanics and Foundations Division, ASCE, Vol. 94, No. SM6, Nov. 1966, pp. 105-134.

4. Seed, H. Bolton and Idriss, I. M., "Analysis of Soil Liquefaction: Niigata Earthquake," Journal of the Soil Mechanics and Foundations Division, ASCE, Vol. 93, No. SM3, May 1967, pp. 83-108. See also Closure Discussion by the authors, same journal 1968.

5. Bishop, A. W., "The Stability of Earth Dams," Ph.D. Thesis, Imperial College, London University, May 1952.

6. Clough, Ray W. and Woodward, Richard J. III, "Analysis of Embankment Stresses and Deformations," Journal of the Soil Mechanics and Foundations Division, ASCE, Vol. 93, No. SM4, July 1967, pp. 529-549.

7. Lowe, John and Karafiath, Leslie, "Stability of Earth Dams Upon Drawdown," Proceedings, 1st PanAmerican Conference on Soil Mechanics, Vol. II, 1960, pp. 537-560.

8. Lee, Kenneth L. and Seed, H. Bolton, "Dynamic Strength of Anisotropically Consolidated Sand," Journal of the Soil Mechanics and Foundations Division, ASCE, Vol. 93, No. SM5, Sept. 1967, pp. 169-190.

9. Seed, H. Bolton, "A Method for Earthquake Resistant Design of Earth Dams," Journal of the Soil Mechanics and Foundations Division, ASCE, Vol. 92, No. SM1, Jan. 1966, pp.13-41.

10. Seed, H. Bolton, Lee, Kenneth L. and Idriss, I. M., "Analysis of the Sheffield Dam Failure," Soil Mechanics and Bituminous Materials Research Laboratory Report, TE 68-2, University of California, Berkeley, April 1968.

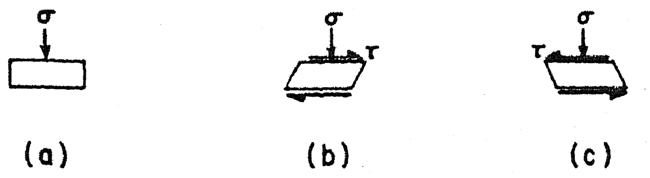

Fig. I IDEALISED STRESS CONDITIONS FOR ELEMENT OF SOIL BELOW GROUND SURFACE DURING AN EARTHQUAKE.

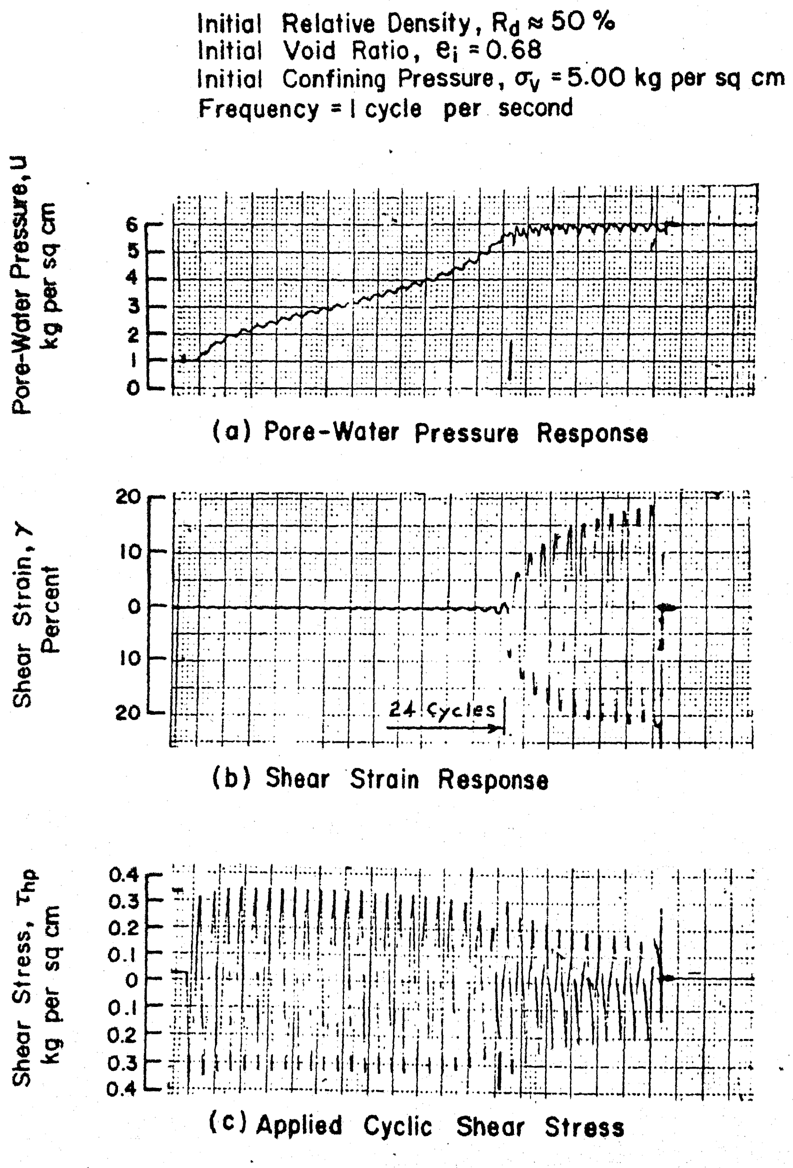

Fig. 2 RECORD OF A TYPICAL PULSATING LOAD TEST ON LOOSE SAND - SIMPLE SHEAR CONDITIONS.

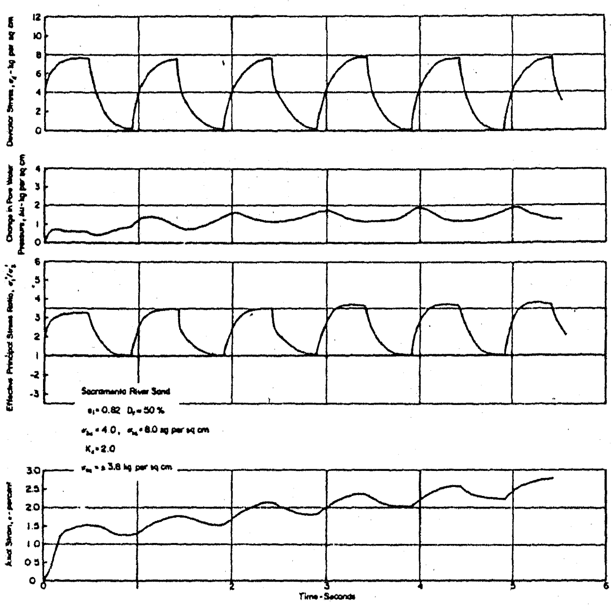

FIG. 3 RESULTS OF THE FIRST 6 SECONDS FROM A TYPICAL PULSATING LOADING TEST ON SATURATED SAND.

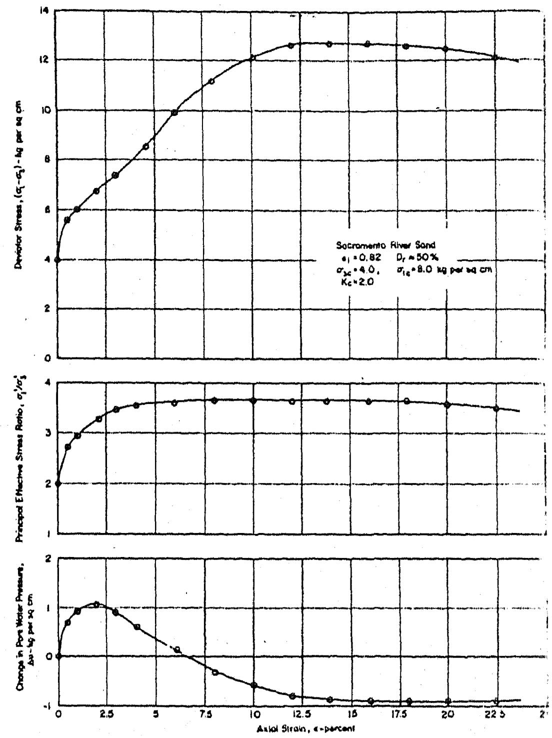

FIG. 4 RESULTS OF STATIC LOADING TEST ON SATURATED SAND

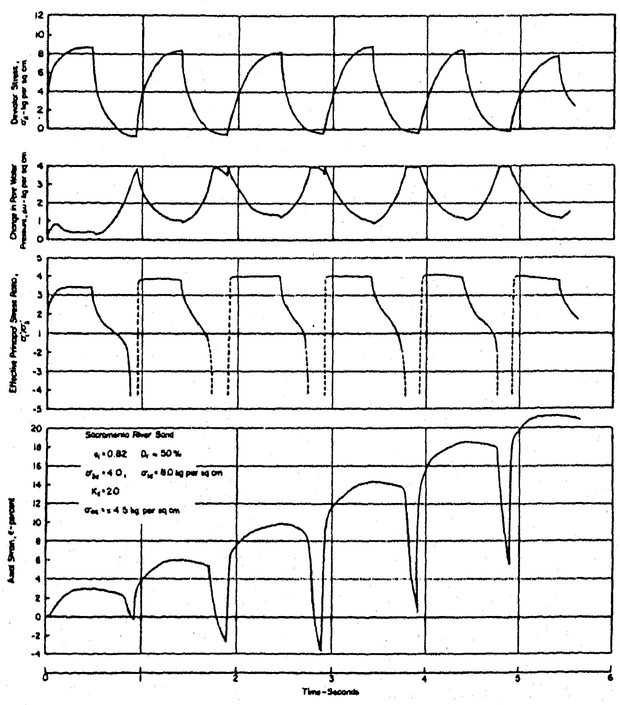

FIG. 5 RESULTS OF CYCLIC LOADING TEST ON SATURATED SAND.

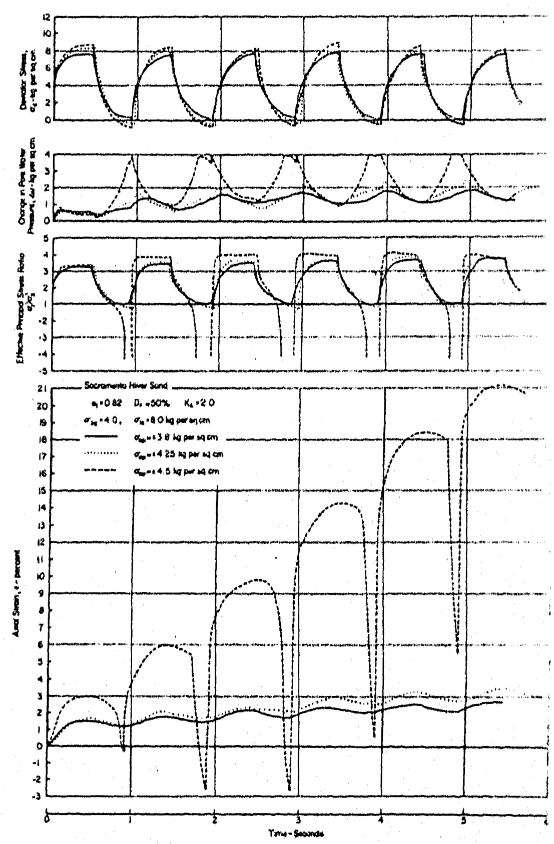

FIG. 6 COMPARISON OF THE RESULTS OF THREE CYCLIC LOADING TESTS ON SATURATED SAND.

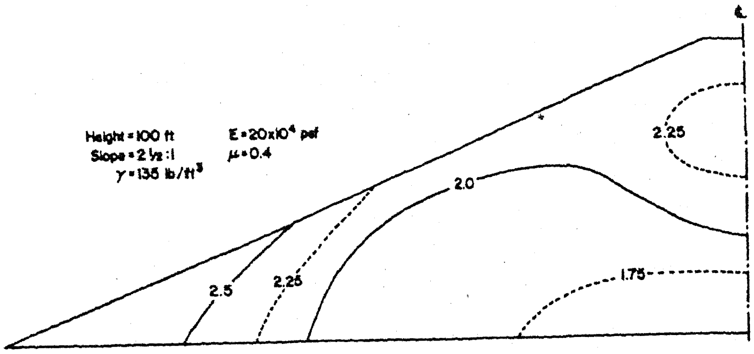

FIG. 7 LINES OF EQUAL PRINCIPAL STRESS RATIO FOR AN EARTH DAM.

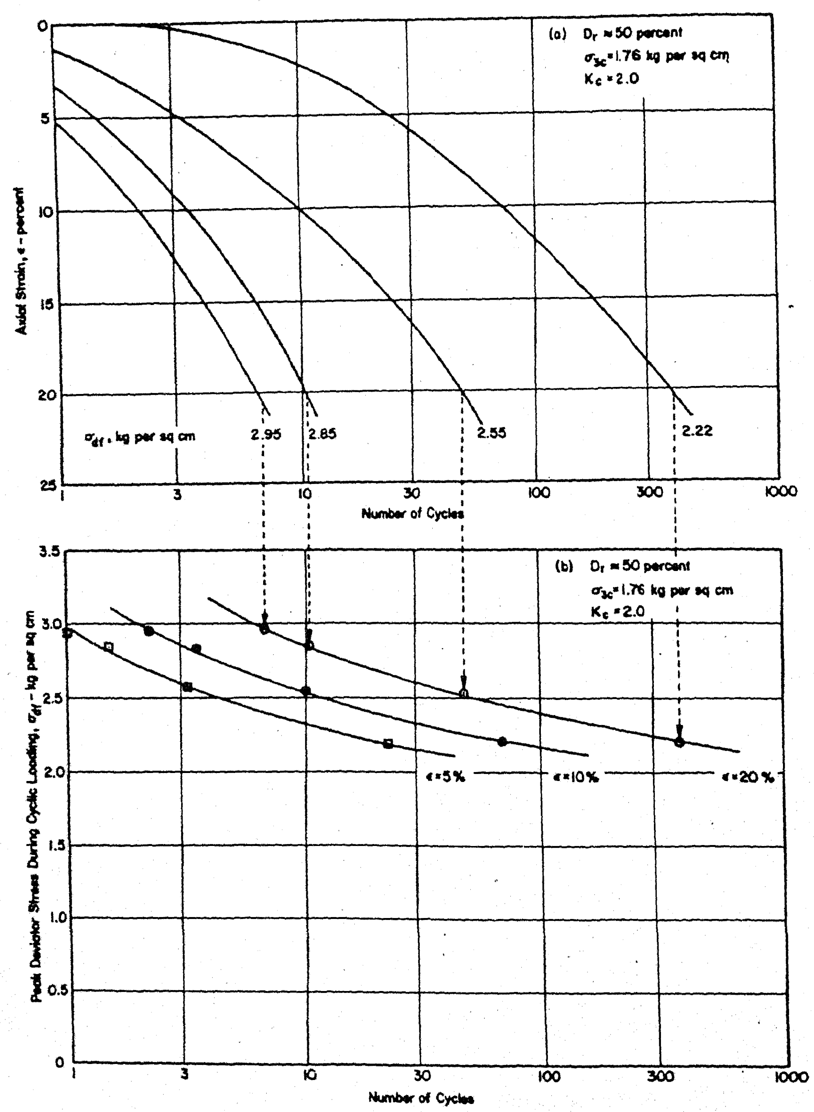

FIG. 8 RESULTS OF A SERIES OF CYCLIC LOADING TESTS ON SILTY SAND HYDRAULIC FILL.

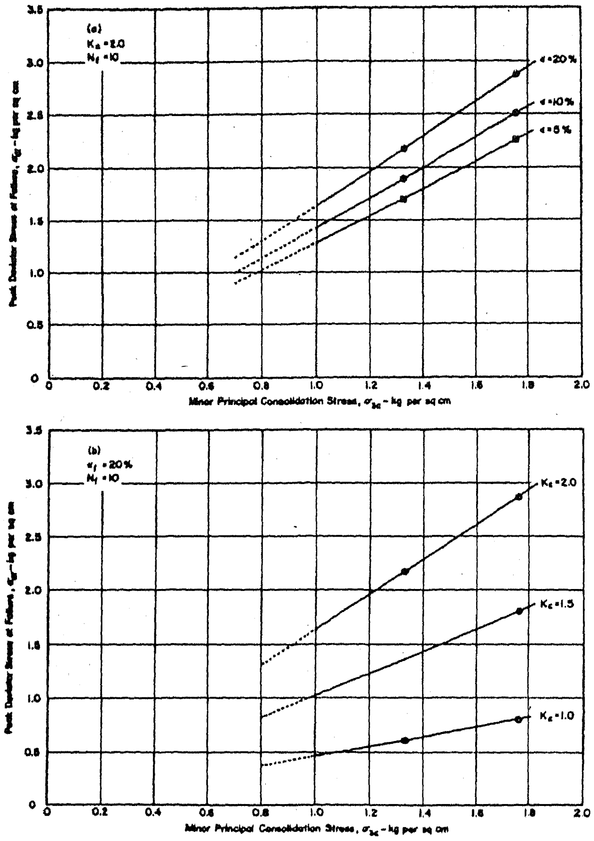

FIG. 9 SUMMARY OF STRENGTHS OBTAINED FROM CYCLIC LOADING TESTS ON SILTY SAND HYDRAULIC FILL.

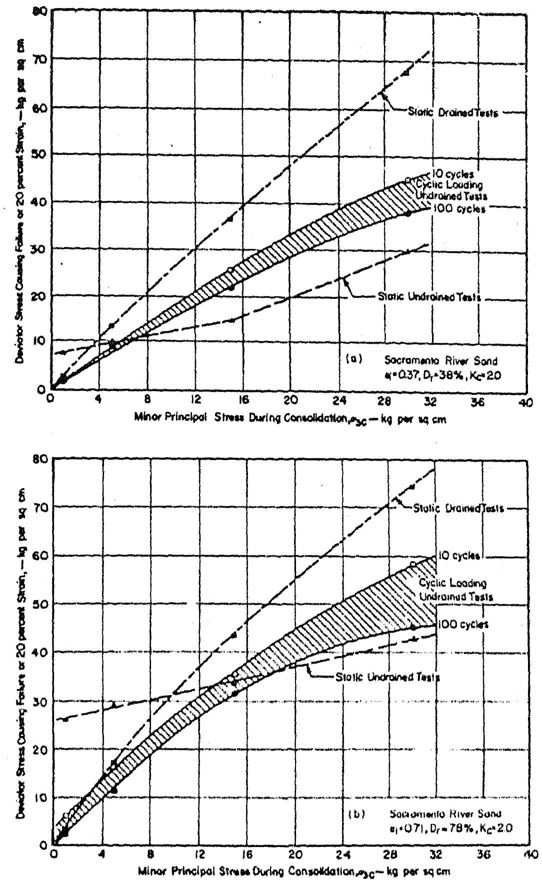

Fig. 11 – COMPARISON OF STATIC AND PULSATING LOADING STRENGTHS AT DIFFERENT DENSITIES AND CONFINING PRESSURES.

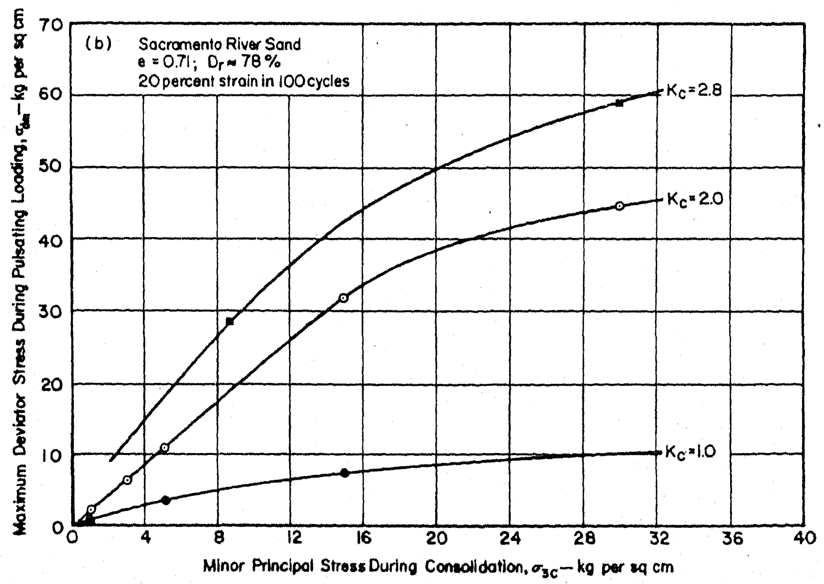

Fig. 10 – PULSATING LOADING STRENGTH AT VARIOUS ANISOTROPIC CONSOLIDATION STRESSES.